Chemi-ionization/recombination processes in the broad-line region of AGNs

Vladimir A. Srećković[1], Milan S. Dimitrijević[2] ,

Ljubinko M. Ignjatović[1]

[1]Institute of Physics, P.O.Box 57, Pregrevica 118, Belgrade, Serbia

[2]Astronomical Observatory, Volgina 7, 11060 Belgrade, Serbia

vlada@ipb.ac.rs

Work done by
Team: prof. Dimitrijevic, Ignjatovic…Institute of physics Belgrade&AOB

Also, we wont to collaborate with experts in AGNs who can help us. Prof. Ilic, Popovic…

Introduction

It is of interest to investigate the influence of the atomic processes in dense parts of BLR clouds and to provide the data useful for modelling and investigations of such layers.

The aim of this investigation is to study the physics of AGN, namely to investigate the atomic processes (collisional atom - Rydberg atom i.e. chemi-ionization/ recombination and also n-n' mixing processes) and revise their role.

In addition, this is particularly significant to better estimate the hydrogen Balmer lines fluxes, which usage for effective temperature diagnostics in astrophysical plasma is limited by errors from the line formation models and uncertainties in used atomic data of hydrogen atom and inelastic collisions.

We wont to find out at what plasma conditions certain atomic processes become important and could explain the existence of AGN regions with such characteristics, and could be used for future diagnostics, numerical simulations and modelling.

Chemi-ionization/recombination processes in the solar photosphere

Short Intro: Solar photosphere and M red dwarf atmosphere, before AGN BLR talk.

Few years ago we started investigations of chemi-ionization/recombination processes and their influence in the solar photosphere.

The Astrophysical Journal Supplement Series, 193:2 (7pp), 2011 March doi:10.1088/0067-0049/193/1/2

CHEMI-IONIZATION IN SOLAR PHOTOSPHERE: INFLUENCE ON THE HYDROGEN ATOM EXCITED STATES POPULATION

Anatolij A. Mihajlov[1,2], Ljubinko M. Ignjatović[1,2], Vladimir A. Srećković[1], and Milan S. Dimitrijević[2,3,4]
[1] Institute of Physics, University of Belgrade, P.O. Box 57, 11001 Belgrade, Serbia; ljuba@ipb.ac.rs, mihajlov@ipb.ac.rs
[2] Isaac Newton Institute of Chile, Yugoslavia Branch, Volgina 7, 11060 Belgrade, Serbia
[3] Astronomical Observatory, Volgina 7, 11060 Belgrade, Serbia
[4] Observatoire de Paris, 92195 Meudon Cedex, France
Received 2010 May 30; accepted 2010 December 5; published 2011 January 18

ABSTRACT

In this paper, the influence of chemi-ionization processes in $H^*(n \geqslant 2) + H(1s)$ collisions, as well as the influence of inverse chemi-recombination processes on hydrogen atom excited-state populations in solar photosphere, are compared with the influence of concurrent electron–atom and electron–ion ionization and recombination processes. It has been found that the considered chemi-ionization/recombination processes dominate over the relevant concurrent processes in almost the whole solar photosphere. Thus, it is shown that these processes and their importance for the non-local thermodynamic equilibrium modeling of the solar atmosphere should be investigated further.

In Mihajlov et al. (2011) we investigated chemi-ionization/recombination processes in H*(n) + H(1s) collisions and their influence on the populations of hydrogen Rydberg atoms and free electrons in weakly ionized layers of the solar photosphere and the lower chromosphere.

We analyse chemi-ionization processes (collisional ionization): 2 channels

$$H^*(n) + H(1s) \Rightarrow H_2^+ + e,$$ Associative chemi-ionization channel i.e. creation of H_2^+ molecular ion.

$$H^*(n) + H(1s) \Rightarrow H(1s) + H^+ + e,$$ Non-associative ionization channel, penning ionization channel

Inverse chemi-recombination processes:

$$H_2^+ + e \Rightarrow H^*(n) + H(1s),$$

$$H(1s) + H^+ + e \Rightarrow H^*(n) + H(1s),$$

We compare with the corresponding electron-atom and other concurent collision processes

$$H^*(n) + e \Rightarrow H^+ + 2e,$$

$$H^+ + 2e \Rightarrow H^*(n) + e,$$

$$H^+ + e \Rightarrow H^*(n) + \varepsilon_\lambda,$$ Ground state

$$A^*(n) + A \Rightarrow A_2^+ + e \qquad (4)$$

$$A^*(n) + A \Rightarrow A + A^+ + e \quad (5)$$

Mechanism of collisional processes (4) and (5) is described in details e.g. in review paper Mihajlov et al. 2012.

A*(n) + A as <u>collisional complex</u> is represented as $[A^+ + A(1s)] + e$ i.e. <u>system of quasi molecule and electron</u>.

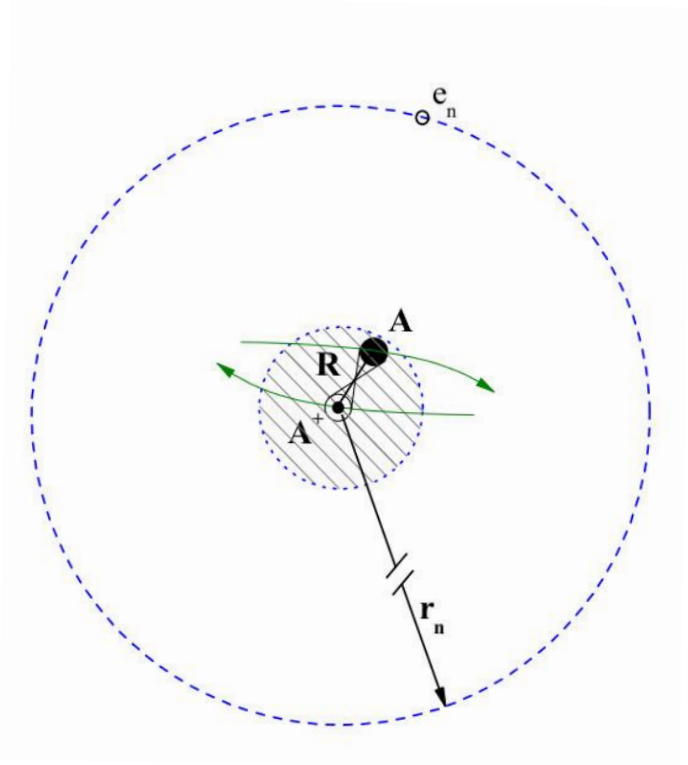

$$A^*(n) + A \Rightarrow A_2^+ + e \qquad (4)$$

$$A^*(n) + A \Rightarrow A + A^+ + e \qquad (5)$$

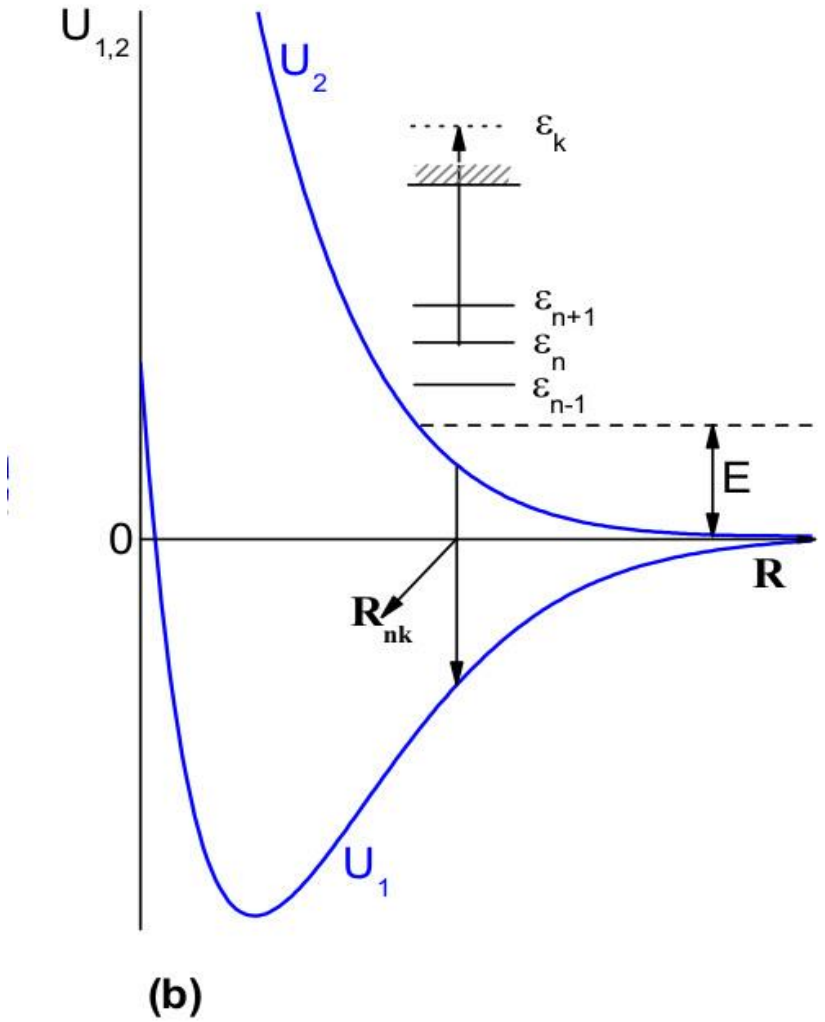

(b)

Using method described e.g. in Mihajlov et al. (2012), we calculated cross sections and rate coefficients for the conditions that exists in weakly ionized layers of the solar photosphere and the lower chromosphere.

$$H^*(n) + H(1s) \Rightarrow H_2^+ + e, \qquad \text{ionization channel a)}$$

$$H^*(n) + H(1s) \Rightarrow H(1s) + H^+ + e, \qquad \text{ionization channel b)}$$

Cross sections for channels a) and b)

$$\sigma_{\mathrm{ci}}^{(a,b)}(n, E) = 2\pi \int_0^{\rho_{\max}^{(a,b)}(E)} P_{\mathrm{ci}}^{(a,b)}(n, \rho, E)\rho d\rho,$$

Rate coefficient for channels a) and b)

$$K_{\mathrm{ci}}^{(a,b)}(n, T) = \int_{E_{\min}^{(a,b)}(n)}^{E_{\max}} v\sigma_{\mathrm{ci}}^{(a,b)}(n, E) f(v; T) dv,$$

Total rate coefficient

$$K_{\mathrm{ci}}(n, T) = K_{\mathrm{ci}}^{(a)}(n, T) + K_{\mathrm{ci}}^{(b)}(n, T),$$

These data are input parameters needed for modeling.

Table 1
Calculated Values of Coefficient K_{ci} ($cm^3\ s^{-1}$) as a Function of n and T

T (K)	n						
	2	3	4	5	6	7	8
4000	0.150E−11	0.619E−09	0.126E−08	0.576E−09	0.554E−09	0.463E−09	0.366E−09
4250	0.202E−11	0.549E−09	0.106E−08	0.617E−09	0.583E−09	0.482E−09	0.378E−09
4500	0.260E−11	0.501E−09	0.900E−09	0.656E−09	0.611E−09	0.500E−09	0.389E−09
4750	0.324E−11	0.488E−09	0.833E−09	0.694E−09	0.637E−09	0.517E−09	0.400E−09
5000	0.403E−11	0.495E−09	0.815E−09	0.730E−09	0.662E−09	0.533E−09	0.410E−09
5250	0.504E−11	0.501E−09	0.800E−09	0.765E−09	0.686E−09	0.548E−09	0.420E−09
5500	0.623E−11	0.500E−09	0.782E−09	0.799E−09	0.709E−09	0.563E−09	0.428E−09
5750	0.756E−11	0.493E−09	0.764E−09	0.832E−09	0.731E−09	0.576E−09	0.437E−09
6000	0.909E−11	0.490E−09	0.757E−09	0.864E−09	0.752E−09	0.589E−09	0.445E−09
6250	0.108E−10	0.502E−09	0.766E−09	0.895E−09	0.772E−09	0.602E−09	0.453E−09
6500	0.128E−10	0.519E−09	0.783E−09	0.924E−09	0.791E−09	0.613E−09	0.460E−09
7000	0.175E−10	0.540E−09	0.808E−09	0.981E−09	0.827E−09	0.635E−09	0.473E−09
7500	0.232E−10	0.574E−09	0.848E−09	0.103E−08	0.860E−09	0.655E−09	0.485E−09
8000	0.300E−10	0.609E−09	0.891E−09	0.108E−08	0.892E−09	0.674E−09	0.497E−09
8500	0.380E−10	0.650E−09	0.939E−09	0.113E−08	0.920E−09	0.691E−09	0.507E−09
9000	0.470E−10	0.688E−09	0.986E−09	0.118E−08	0.948E−09	0.707E−09	0.516E−09
9500	0.574E−10	0.733E−09	0.104E−08	0.122E−08	0.973E−09	0.722E−09	0.525E−09
10000	0.689E−10	0.787E−09	0.109E−08	0.126E−08	0.997E−09	0.736E−09	0.533E−09

Table 2
Calculated Values of Recombination Coefficient K_{cr} ($cm^6\ s^{-1}$) as a Function of n and T

T (K)	n						
	2	3	4	5	6	7	8
4000	0.190E−27	0.732E−27	0.390E−27	0.114E−27	0.977E−28	0.831E−28	0.709E−28
4250	0.130E−27	0.458E−27	0.257E−27	0.102E−27	0.880E−28	0.753E−28	0.645E−28
4500	0.918E−28	0.305E−27	0.177E−27	0.914E−28	0.799E−28	0.688E−28	0.591E−28
4750	0.666E−28	0.223E−27	0.135E−27	0.828E−28	0.730E−28	0.631E−28	0.544E−28
5000	0.506E−28	0.174E−27	0.110E−27	0.755E−28	0.671E−28	0.582E−28	0.503E−28
5250	0.403E−28	0.138E−27	0.912E−28	0.693E−28	0.619E−28	0.540E−28	0.467E−28
5500	0.331E−28	0.111E−27	0.763E−28	0.639E−28	0.575E−28	0.502E−28	0.436E−28
5750	0.275E−28	0.889E−28	0.645E−28	0.592E−28	0.535E−28	0.469E−28	0.407E−28
6000	0.233E−28	0.731E−28	0.558E−28	0.551E−28	0.500E−28	0.440E−28	0.382E−28
6250	0.201E−28	0.627E−28	0.498E−28	0.514E−28	0.469E−28	0.413E−28	0.360E−28
6500	0.176E−28	0.548E−28	0.451E−28	0.482E−28	0.441E−28	0.389E−28	0.339E−28
7000	0.139E−28	0.421E−28	0.374E−28	0.427E−28	0.393E−28	0.348E−28	0.304E−28
7500	0.114E−28	0.341E−28	0.322E−28	0.382E−28	0.354E−28	0.314E−28	0.275E−28
8000	0.964E−29	0.284E−28	0.283E−28	0.345E−28	0.321E−28	0.286E−28	0.250E−28
8500	0.834E−29	0.243E−28	0.253E−28	0.314E−28	0.293E−28	0.261E−28	0.229E−28
9000	0.731E−29	0.211E−28	0.229E−28	0.287E−28	0.269E−28	0.240E−28	0.211E−28
9500	0.654E−29	0.187E−28	0.209E−28	0.264E−28	0.248E−28	0.222E−28	0.195E−28
10000	0.590E−29	0.169E−28	0.194E−28	0.245E−28	0.230E−28	0.206E−28	0.181E−28

The <u>first conclusion</u> from the paper Mihajlov et al. (2011) relates to relative contribution of partial chemi-ionization/recombination processes i.e. channels a) and b) for given *n* and *T*

Info about H_2^+ molecule presence

Table 3
Calculated Values of Coefficient $X^{(a)} \equiv K_{ci}^{(a)}/K_{ci} = K_{cr}^{(a)}/K_{cr}$ as a Function of n and T

T (K)	n						
	2	3	4	5	6	7	8
4000	0.998	0.955	0.877	0.507	0.408	0.335	0.281
4250	0.969	0.934	0.827	0.484	0.388	0.318	0.266
4500	0.924	0.907	0.765	0.463	0.371	0.303	0.254
4750	0.872	0.881	0.709	0.443	0.354	0.289	0.242
5000	0.819	0.857	0.664	0.425	0.339	0.277	0.231
5250	0.769	0.831	0.619	0.408	0.325	0.265	0.221
5500	0.721	0.800	0.568	0.393	0.312	0.254	0.212
5750	0.673	0.764	0.515	0.378	0.300	0.244	0.203
6000	0.627	0.728	0.466	0.364	0.288	0.235	0.196
6250	0.585	0.699	0.430	0.351	0.278	0.226	0.188
6500	0.546	0.672	0.399	0.339	0.268	0.218	0.182
7000	0.474	0.610	0.336	0.317	0.250	0.204	0.169
7500	0.414	0.558	0.289	0.297	0.235	0.190	0.158
8000	0.363	0.510	0.250	0.280	0.221	0.179	0.149
8500	0.321	0.469	0.220	0.264	0.208	0.169	0.141
9000	0.287	0.429	0.193	0.250	0.197	0.160	0.133
9500	0.258	0.398	0.174	0.237	0.187	0.151	0.126
10000	0.234	0.376	0.160	0.225	0.177	0.144	0.120

$$H^*(n) + H(1s) \Rightarrow H_2^+ + e, \qquad \text{(a)}$$

$$H^*(n) + H(1s) \Rightarrow H(1s) + H^+ + e, \qquad \text{(b)}$$

branch coefficients ratio

$$X_{ci}^{(a,b)}(n,T) = \frac{K_{ci}^{(a,b)}(n,T)}{K_{ci}(n,T)},$$

Second conclusion relates to the comparison with the corresponding electron-atom collision processes

Comparison of Fluxes of the Considered Processes

$$I_{ci}(n,T) = K_{ci}(n,T) \cdot N_n N_1,$$
$$I_{cr}(n,T) = K_{cr}(n,T) \cdot N_1 N_i N_e,$$

$$I_{i;ea}(n,T) = K_{ea}(n,T) \cdot N_n N_e,$$
$$I_{r;eci}(n,T) = K_{eci}(n,T) \cdot N_i N_e N_e,$$
$$I_{r;ph}(n,T) = K_{ph}(n,T) \cdot N_i N_e,$$

Quantity F(n,T) i.e. ratio of fluxes. Partial, for every *n*

$$F_i(n,T) = \frac{I_{ci}(n,T)}{I_{i;ea}(n,T)} = \frac{K_{ci}(n,T)}{K_{ea}(n,T)} \cdot N_1 N_e,$$

Total, for the whole block of the excited hydrogen atom states with $2 \le n \le 8$

$$F_{i,ea;2-8}(T) = \frac{\sum_{n=2}^{8} I_{ci}(n,T)}{\sum_{n=2}^{8} I_{i;ea}(n,T)}$$

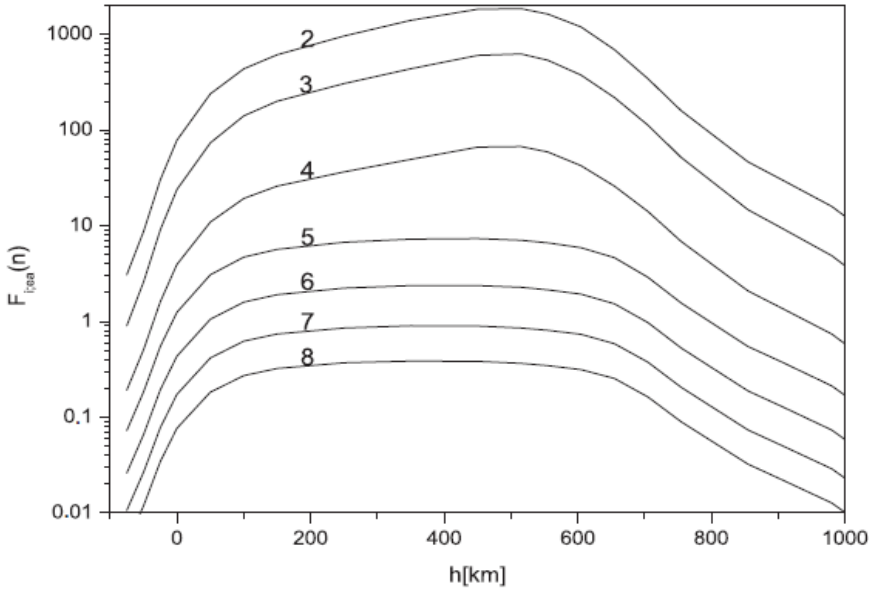

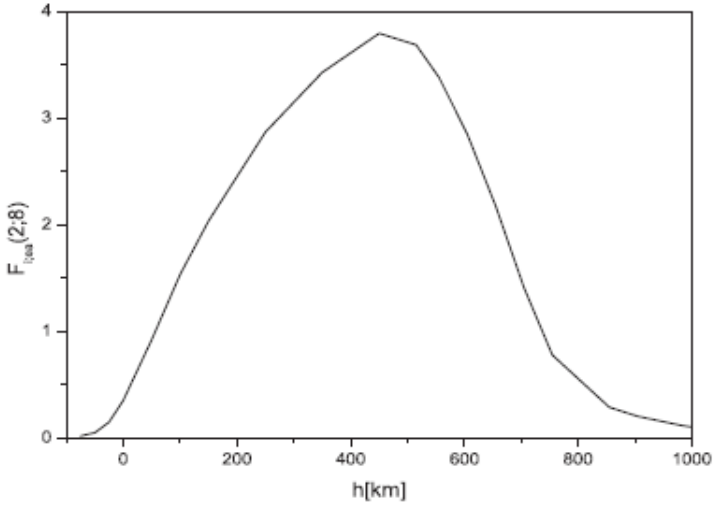

Figure 4. Behavior of the quantity $F_{i;ea}(2;8)$ given by Equation (29), as a function of height *h*.

It has been demonstrated in Mihajlov et al. (2011) that chemi-ionization/ recombination processes in H(n) + H(1s) collisions, for the principal quantum number n>2, must have significant influence in comparison with the corresponding electron-atom collision processes on the populations of hydrogen Rydberg atoms and electrons in weakly ionized layers of the solar photosphere and the lower chromosphere, and that they have to be included in modelling and investigation of solar plasma, especially in the region of the temperature minimum in the Solar photosphere. And should influence on the atomic spectral line shapes.

functions of height (*h*) in solar photosphere

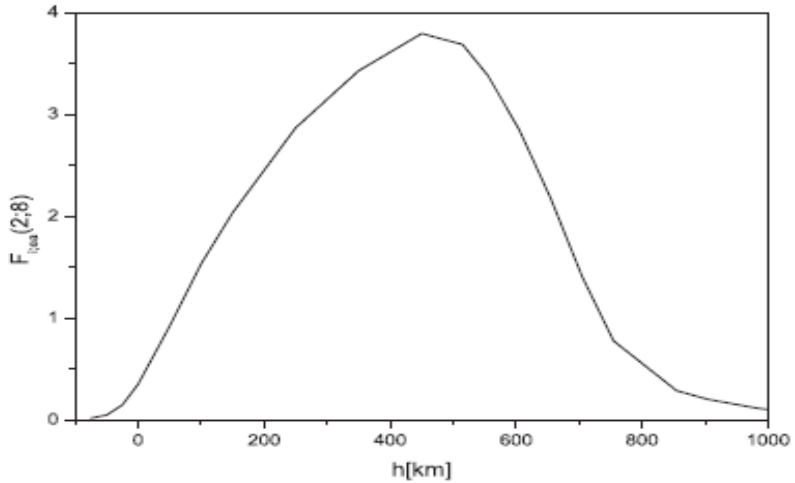

Figure 4. Behavior of the quantity $F_{i;ea}(2; 8)$ given by Equation (29), as a function of height h.

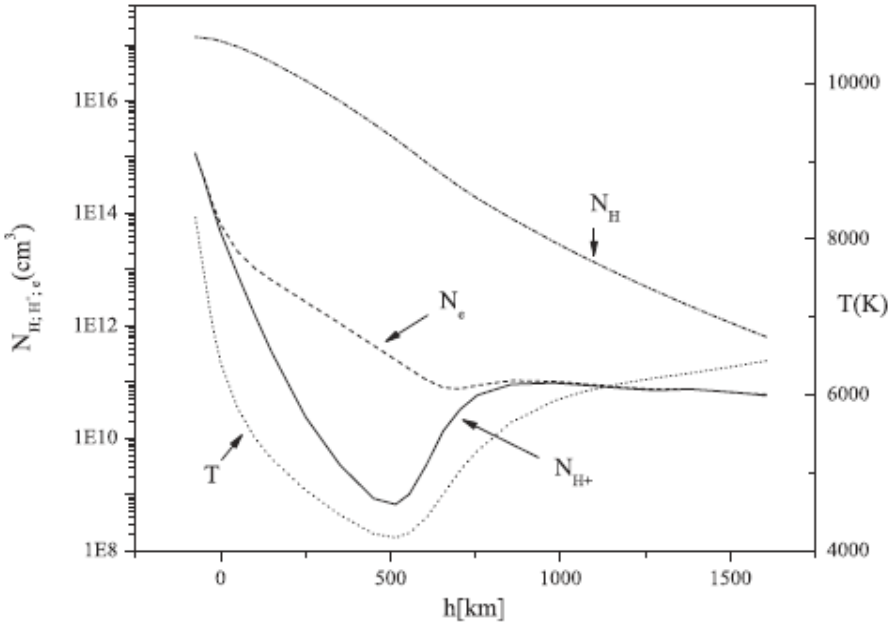

Figure 1. Basic plasma parameters, for the solar model of Vernazza et al. (1981), as a function of height h.

Next result:

M red dwarf atmosphere with the effective temperature T_{eff} = 3800 K

Contents lists available at ScienceDirect

New Astronomy Reviews

journal homepage: www.elsevier.com/locate/newastrev

Rydberg atoms in astrophysics

Yu.N. Gnedin [a], A.A. Mihajlov [b], Lj.M. Ignjatović [b], N.M. Sakan [b], V.A. Srećković [b,*], M.Yu. Zakharov [c], N.N. Bezuglov [c], A.N. Klycharev [c]

[a] Central Astronomical Observatory, Pulkovo, RAS, Russia
[b] Institute of Physics, P.O. Box 57, 11001 Belgrade, Serbia
[c] Department of Physics, Saint-Petersburg University, Ulianovskaya 1, 198504 St. Petersburg, Petrodvorets, Russia

The results suggest that the chemi-ionization/recombination processes due to their influence on the excited state populations and the free electron density, also should influence on the atomic spectral line shapes.

This assumption is confirmed by the Figs, which show the profiles of some of hydrogen spectral lines in the M red stars calculated with and without these processes using PHOENIX code.

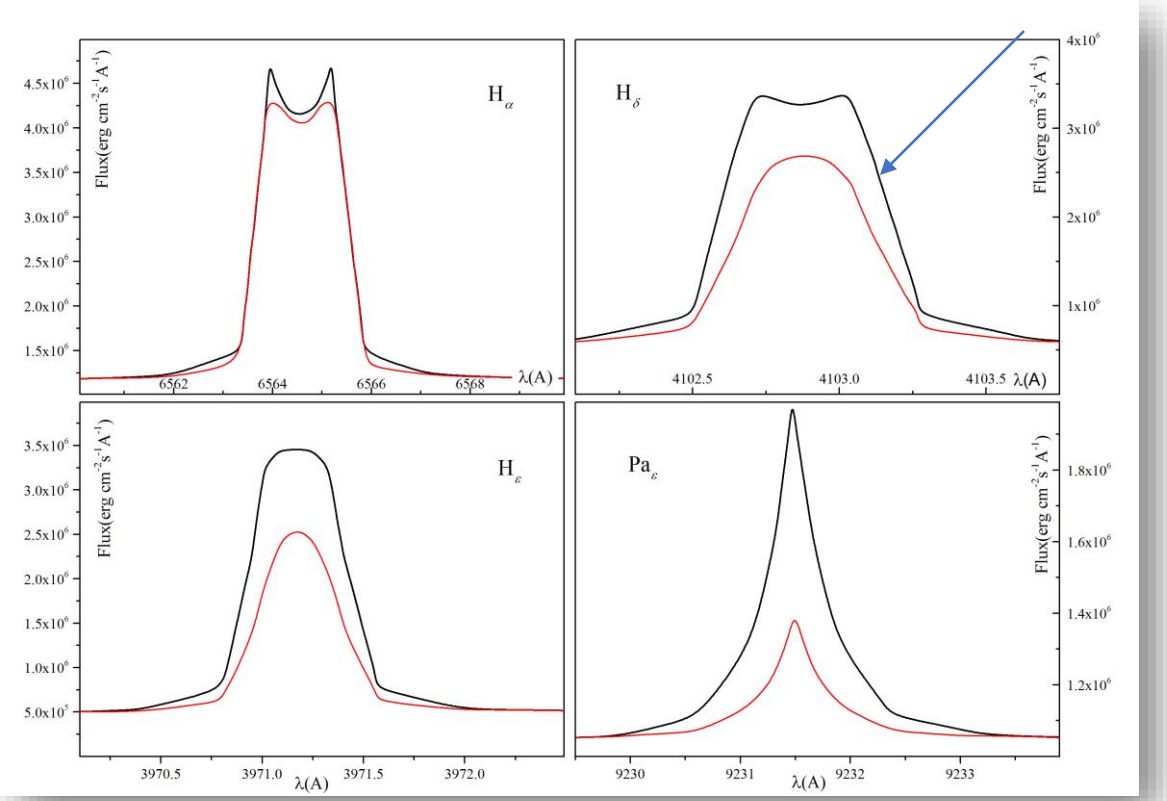

Figure 13 (from [26]) show the line profiles of H_α, H_δ, H_ϵ Pa_ϵ with and without inclusion of processes (1). Profiles are synthesized with PHOENIX code with Stark broadening contribution calculated using tables from [40] for Stark broadening of hydrogen lines (linear Stark effect). Lineshape changes, especially in the wings, show the influence of the electron density change having a direct influence on the Stark broadening of hydrogen lines.

Let's go back to the chemi-ionization/recombination atomic processes in the AGNs broad-line region

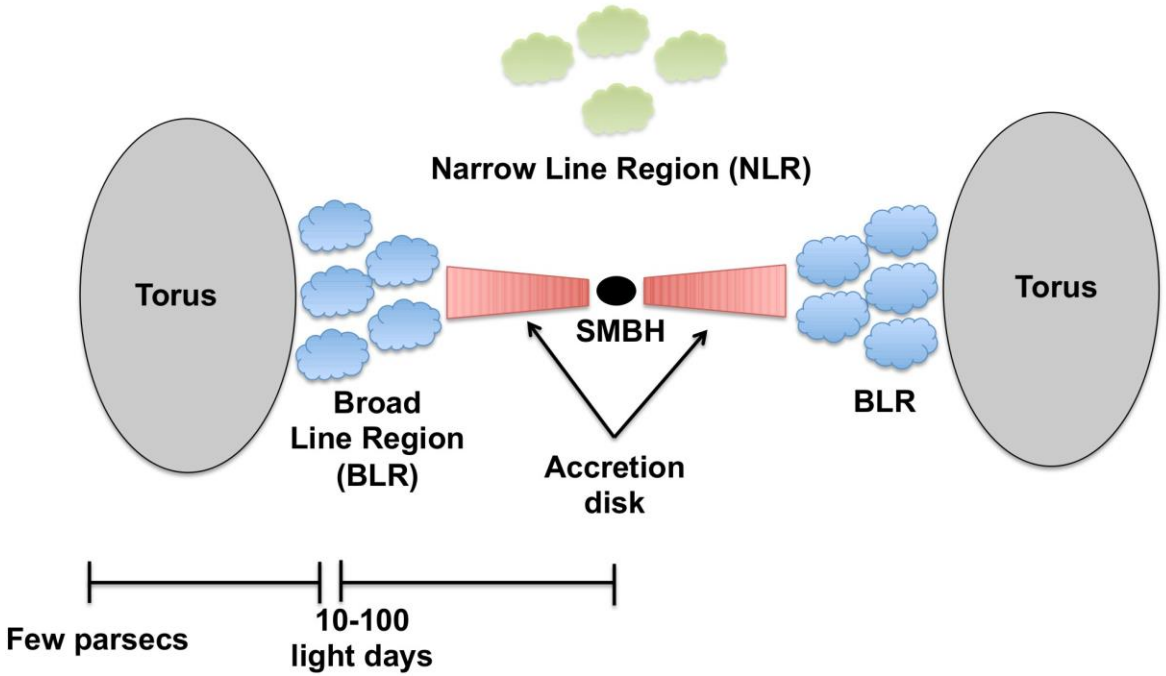

Out main idea

In AGN, especially in the region of the moderately ionized layers of dense parts of the BLR clouds plasma conditions are closer to stellar atmospheres than to photoionized nebulae (Osterbrock 1989).

Consequently, it is of interest to investigate the influence of the mentioned processes in dense parts of BLR clouds and to provide the data on the corresponding rate coefficients useful for modelling and investigations of such layers.

That is conlusion of papers Netzer 1990; Jogee 2006; Osterbrock & Ferland 2006 :

In order to develop and improve diagnostic methods needed for the estimation of the physical conditions in the particular parts of active galactic nuclei (AGNs), the investigation of the influence of various relevant atomic and molecular collisional processes is **needed**.

we started to check the literature. problems

Paper of Mercè Crosas and Jon C. Weisheit, *Hydrogen molecules in quasar broad-line regions*, MNRAS, 1993, 262, 359.

they report uncertainties of the rate coefficients due to hydrogen collisions in almost all cases.

CI: No rate coefficients for higher *n (n>3)* and no rate coefficients for second non-associative channel.

For the conditions 10^4 - 10^{10} cm^{-3} they concluded that the influence of the associative chemi -ionization processes is negligible in BLR clouds.

However, we assume that in very dense weakly ionized regions with > 10^{10} cm^{-3} (if exists), these chemi ionization/ recombination processes could be important and could change the optical characteristics.

Table 2. Collisional reactions.

	Reaction	Rate Coefficient (cm^3/s)		Ref
1.	$H^+ + e^- \rightarrow H + h\nu$	$K_1 = 1.59 \times 10^{-13} T_4^{-0.5} e^{-\tau_{LL}} + 2.6 \times 10^{-13} T_4^{-0.85}$		1
2.	$H + e^- \rightarrow H^- + h\nu$	$K_2 = 2.65 \times 10^{-15} T_4 + 1.22 \times 10^{-15}$		2
3.	$H^- + H \rightarrow H_2 + e^-$	$K_3 = 2.7 \times 10^{-9}$		3
4.	$H^- + H^+ \rightarrow H + H$	$K_4 = 7.0 \times 10^{-9} T_4^{-0.5}$		4
5.	$H^- + H_2^+ \rightarrow H + H + H$ $\rightarrow H_2 + H$	$K_5 = 5.0 \times 10^{-8} T_4^{-0.5}$		4
6.	$H^+ + H \rightarrow H_2^+ + h\nu$	$K_6 = 2.9 \times 10^{-16} T_4^{-1.8}$,	$T < 6700K$	5
		$K_6 = 5.8 \times 10^{-16} (T_4/5.6)^{-0.66 \log 10(T_4/5.6)}$,	$T > 6700K$	5
7.	$H_2^+ + H \rightarrow H_2 + H^+$	$K_7 = 6.4 \times 10^{-10}$		6
8.	$H_2 + H^+ \rightarrow H_2^+ + H$	$K_8 = 2.4 \times 10^{-9} e^{-2.12/T_4}$		7
9.	$H_2^+ + e^- \rightarrow H^+ + H + e^-$	$K_9 = 2.0 \times 10^{-8}$		8
10.	$H_2 + e^- \rightarrow 2H + e^-$	$K_{10} = 1.1 \times 10^{-8} e^{-10.2/T_4} T_4^{0.35}$		5
11.	$H_2 + e^- \rightarrow H^- + H$	$K_{11} = 9.69 \times 10^{-13} e^{-11.323/(\ln 10^4 T_4 - 7.28)}$		5
12.	$H + H + H \rightarrow H_2 + H$	$K_{12} = 5.5 \times 10^{-33} T_4^{-1}$		5
13.	$H_2 + H \rightarrow H + H + H$	$K_{13} = 6.53 \times 10^{-9} e^{-5.24/T_4}$		5
14.	$H_2 + H + H \rightarrow H_2 + H_2$	$K_{13} = K_{10}/8$		5
15.	$H_2 + H_2 \rightarrow H_2 + H + H$	$K_{15} = 11.3 \times 10^{-9} e^{-5.33/T_4}$		5
16.	$H(n=1) + H^*(n=2) \rightarrow H_2^* \rightarrow H_2 + h\nu$	$K_{16} = 5.0 \times 10^{-14}$		9
17.	$H(n=1) + H^*(n=2) \rightarrow H_2^+ + e^-$	$K_{17} = 8.73 \times 10^{-12} T_4^{0.95}$,	$T < 5000K$	10
		$K_{17} = 2.9 \times 10^{-11} T_4^{2.69}$,	$T > 5000K$	10
18.	$H(n=1) + H^*(n=3) \rightarrow H_2^+ + e^-$	$K_{18} = 4.42 \times 10^{-11} T_4^{0.95} e^{0.87/T_4}$,	$T < 5000K$	11
		$K_{18} = 1.47 \times 10^{-10} T_4^{2.69} e^{0.87/T_4}$,	$T > 5000K$	11

For example in Marziani et al. (2011), Negrete et al. (2012) and Marziani et al. (2015), hydrogen atom density $7.00 \leq \log n_H \leq 14.00$ has been used for various simulations in BLR with the code CLOUDY (Ferland et al. 2013). Higher densities exists.

On the other hand, the illuminated surface of the BLR clouds is highly ionized, but if they are sufficiently large the temperature may decrease to the much lower values, e.g. up to around 2000 K, as was taken in Crosas &Weisheit (1993), where gas is weakly ionized with large amount of hydrogen molecules (Crosas & Weisheit 1993).

If very dense weakly ionized regions exist, these chemi-ionization/ recombination processes could be important and could change the optical characteristics.

there is a need for accurate data

$$\sigma_{\mathrm{ci}}^{(a,b)}(n, E) = 2\pi \int_0^{\rho_{\max}^{(a,b)}(E)} P_{\mathrm{ci}}^{(a,b)}(n, \rho, E)\rho d\rho,$$

$$K_{\mathrm{ci}}^{(a,b)}(n, T) = \int_{E_{\min}^{(a,b)}(n)}^{E_{\max}} v\sigma_{\mathrm{ci}}^{(a,b)}(n, E) f(v; T) dv,$$

$$K_{\mathrm{ci}}(n, T) = K_{\mathrm{ci}}^{(a)}(n, T) + K_{\mathrm{ci}}^{(b)}(n, T),$$

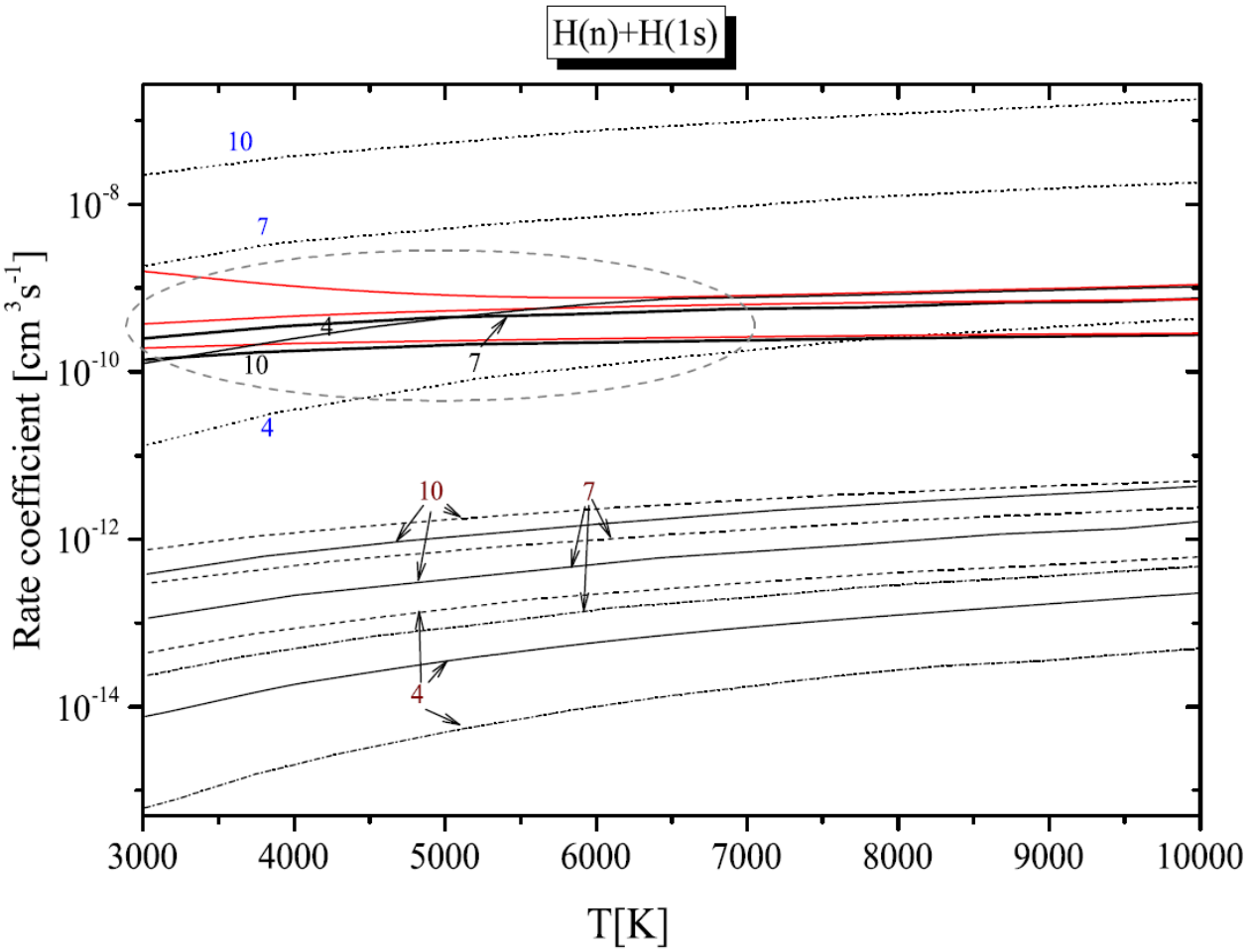

Figure 2. Plot of collisional ionization H(n) + H(1s) rate coefficients for selected excited states (n = 4, 7, 10). The black lines are the data analysed in Barklem (2007) for non-associative channel (4), where A = H. The data from

Literature: the uncertainties of the rate coefficients in hydrogen collision. Differences, almost few order of magnitudes from different sources.

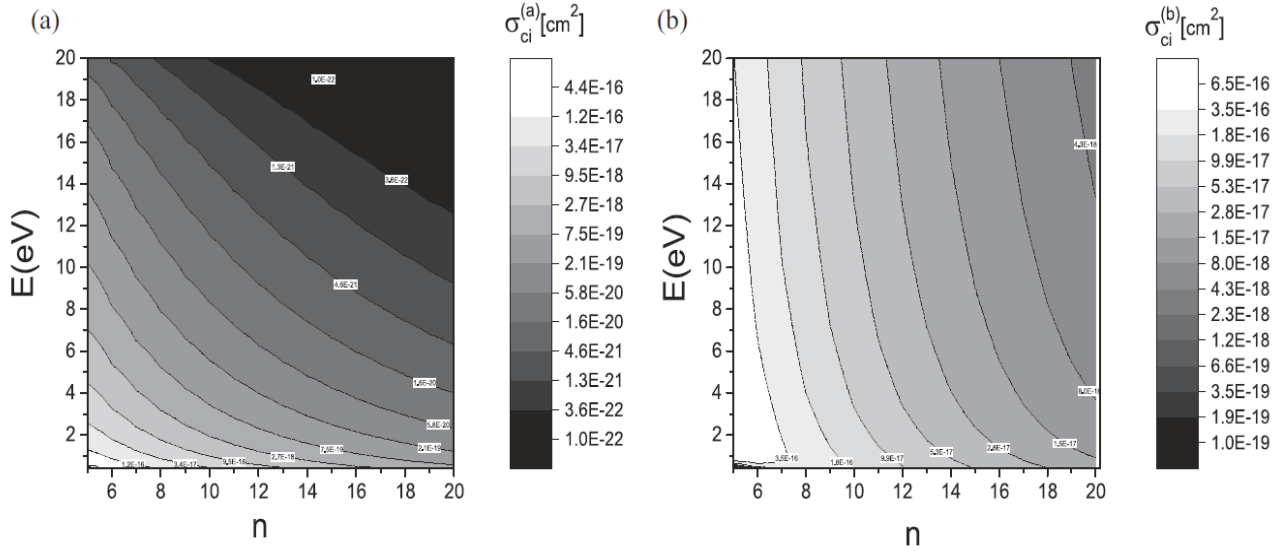

Figure 1. (a) The surface plot of the partial cross-section $\sigma_{ci}^{(a)}(n, E)$ equation (10) of the chemi-ionization processes (3), i.e. associative ionization channel. (b) The surface plot of the partial cross-sections $\sigma_{ci}^{(b)}(n, E)$ equation (10) of the chemi-ionization processes (4), i.e. non-associative ionization channel.

Table 3. Calculated Values of Coefficient K_{ci}[cm^3/s] as a function of n and T ($2 \le n \le 10$ and 3000 K $\le T \le$ 20000 K). The values for $2 \le n \le 8$ and 4000 K $\le T \le$ 10000 K are from Mihajlov et al. (2011) and here are given for integrity.

T/n	2	3	4	5	6	7	8	9	10
3000	9.20E-13	7.32E-10	1.61E-09	3.99E-10	4.21E-10	3.73E-10	3.06E-10	2.44E-10	1.92E-10
3500	1.10E-12	6.90E-10	1.57E-09	4.90E-10	4.91E-10	4.21E-10	3.38E-10	2.65E-10	2.06E-10
4000	1.50E-12	6.19E-10	1.26E-09	5.76E-10	5.54E-10	4.63E-10	3.66E-10	2.83E-10	2.17E-10
4500	2.60E-12	5.01E-10	9.00E-10	6.56E-10	6.11E-10	5.00E-10	3.89E-10	2.98E-10	2.28E-10
5000	4.03E-12	4.95E-10	8.15E-10	7.30E-10	6.62E-10	5.33E-10	4.10E-10	3.11E-10	2.36E-10
5500	6.23E-12	5.00E-10	7.82E-10	7.99E-10	7.09E-10	5.63E-10	4.28E-10	3.23E-10	2.44E-10
6000	9.09E-12	4.90E-10	7.57E-10	8.64E-10	7.52E-10	5.89E-10	4.45E-10	3.33E-10	2.51E-10
6500	1.28E-11	5.19E-10	7.83E-10	9.24E-10	7.91E-10	6.13E-10	4.60E-10	3.42E-10	2.56E-10
7000	1.75E-11	5.40E-10	8.08E-10	9.81E-10	8.27E-10	6.35E-10	4.73E-10	3.51E-10	2.62E-10
7500	2.32E-11	5.74E-10	8.48E-10	1.03E-09	8.60E-10	6.55E-10	4.85E-10	3.58E-10	2.67E-10
8000	3.00E-11	6.09E-10	8.91E-10	1.08E-09	8.92E-10	6.74E-10	4.97E-10	3.65E-10	2.71E-10
8500	3.80E-11	6.50E-10	9.39E-10	1.13E-09	9.20E-10	6.91E-10	5.07E-10	3.72E-10	2.75E-10
9000	4.70E-11	6.88E-10	9.86E-10	1.18E-09	9.48E-10	7.07E-10	5.16E-10	3.77E-10	2.79E-10
9500	5.74E-11	7.33E-10	1.04E-09	1.22E-09	9.73E-10	7.22E-10	5.25E-10	3.83E-10	2.82E-10
10000	6.89E-11	7.87E-10	1.09E-09	1.26E-09	9.97E-10	7.36E-10	5.33E-10	3.88E-10	2.85E-10
11000	9.47E-11	7.49E-10	1.31E-09	1.33E-09	1.04E-09	7.61E-10	5.48E-10	3.97E-10	2.91E-10
12000	1.25E-10	8.39E-10	1.41E-09	1.40E-09	1.08E-09	7.83E-10	5.61E-10	4.05E-10	2.96E-10
13000	1.59E-10	9.29E-10	1.51E-09	1.46E-09	1.11E-09	8.03E-10	5.73E-10	4.12E-10	3.00E-10
14000	1.95E-10	1.02E-09	1.60E-09	1.52E-09	1.15E-09	8.21E-10	5.83E-10	4.18E-10	3.04E-10
15000	2.35E-10	1.11E-09	1.68E-09	1.57E-09	1.18E-09	8.37E-10	5.92E-10	4.23E-10	3.08E-10
16000	2.76E-10	1.20E-09	1.77E-09	1.62E-09	1.20E-09	8.52E-10	6.01E-10	4.29E-10	3.11E-10
17000	3.19E-10	1.28E-09	1.84E-09	1.66E-09	1.23E-09	8.65E-10	6.08E-10	4.33E-10	3.14E-10
18000	3.63E-10	1.37E-09	1.92E-09	1.71E-09	1.25E-09	8.78E-10	6.16E-10	4.37E-10	3.16E-10
19000	4.08E-10	1.45E-09	1.99E-09	1.74E-09	1.27E-09	8.89E-10	6.22E-10	4.41E-10	3.19E-10
20000	4.55E-10	1.53E-09	2.06E-09	1.78E-09	1.29E-09	9.00E-10	6.28E-10	4.45E-10	3.21E-10

Extended calc.

n →

T ↓

Table 1. Calculated Values of Coefficient K_{ci}[$cm^3\ s^{-1}$] as a function of n and T. A portion is shown here for guidance regarding its form and content.

T/n	10	11	12	13	14	15	16	17	18	19	20
3000	1.92E-10	1.51E-10	1.19E-10	9.44E-11	7.56E-11	6.11E-11	4.98E-11	4.09E-11	3.39E-11	2.82E-11	2.37E-11
4000	2.17E-10	1.68E-10	1.31E-10	1.03E-10	8.19E-11	6.57E-11	5.32E-11	4.35E-11	3.58E-11	2.97E-11	2.49E-11
5000	2.36E-10	1.81E-10	1.40E-10	1.09E-10	8.62E-11	6.88E-11	5.55E-11	4.52E-11	3.72E-11	3.08E-11	2.57E-11
6000	2.51E-10	1.90E-10	1.46E-10	1.14E-10	8.94E-11	7.12E-11	5.73E-11	4.65E-11	3.82E-11	3.16E-11	2.63E-11
7000	2.62E-10	1.98E-10	1.51E-10	1.17E-10	9.20E-11	7.30E-11	5.86E-11	4.76E-11	3.89E-11	3.22E-11	2.68E-11
8000	2.71E-10	2.04E-10	1.55E-10	1.20E-10	9.40E-11	7.45E-11	5.97E-11	4.84E-11	3.96E-11	3.26E-11	2.72E-11
9000	2.79E-10	2.09E-10	1.59E-10	1.22E-10	9.57E-11	7.57E-11	6.06E-11	4.90E-11	4.01E-11	3.30E-11	2.75E-11
10000	2.85E-10	2.13E-10	1.62E-10	1.24E-10	9.71E-11	7.67E-11	6.14E-11	4.96E-11	4.05E-11	3.34E-11	2.77E-11
11000	2.91E-10	2.17E-10	1.64E-10	1.26E-10	9.83E-11	7.76E-11	6.20E-11	5.01E-11	4.09E-11	3.36E-11	2.79E-11
12000	2.96E-10	2.20E-10	1.66E-10	1.28E-10	9.93E-11	7.83E-11	6.25E-11	5.05E-11	4.12E-11	3.39E-11	2.81E-11
13000	3.00E-10	2.23E-10	1.68E-10	1.29E-10	1.00E-10	7.90E-11	6.30E-11	5.09E-11	4.14E-11	3.41E-11	2.83E-11
14000	3.04E-10	2.25E-10	1.70E-10	1.30E-10	1.01E-10	7.96E-11	6.35E-11	5.12E-11	4.17E-11	3.43E-11	2.84E-11
15000	3.08E-10	2.28E-10	1.71E-10	1.31E-10	1.02E-10	8.01E-11	6.38E-11	5.15E-11	4.19E-11	3.44E-11	2.86E-11
16000	3.11E-10	2.30E-10	1.73E-10	1.32E-10	1.02E-10	8.06E-11	6.42E-11	5.17E-11	4.21E-11	3.46E-11	2.87E-11
17000	3.14E-10	2.31E-10	1.74E-10	1.33E-10	1.03E-10	8.10E-11	6.45E-11	5.19E-11	4.23E-11	3.47E-11	2.88E-11
18000	3.16E-10	2.33E-10	1.75E-10	1.34E-10	1.04E-10	8.14E-11	6.48E-11	5.21E-11	4.24E-11	3.48E-11	2.89E-11
19000	3.19E-10	2.35E-10	1.76E-10	1.34E-10	1.04E-10	8.17E-11	6.50E-11	5.23E-11	4.26E-11	3.50E-11	2.90E-11
20000	3.21E-10	2.36E-10	1.77E-10	1.35E-10	1.04E-10	8.20E-11	6.52E-11	5.25E-11	4.27E-11	3.51E-11	2.90E-11

In order to enable the better and more adequate use of data, we give for the rate coefficients a simple and accurate fitting formula based on a least-squares method, which is logarithmic and represented by a second-degree polynomial

$$\log(K_{ci}(T)) = k_1 + k_2 \log(T) + k_3 (\log(T))^2.$$

Table 2. The fits of the equation (13) to the rate coefficient. A portion is shown here for guidance regarding its form.

n	k_1	k_2	k_3
4	19.91758	– 15.14785	1.98009
5	– 20.60455	5.21174	– 0.57122
6	– 17.85054	3.94548	– 0.43315
7	– 16.16158	3.1383	– 0.34519
8	– 15.03989	2.57737	– 0.28382
9	– 14.20649	2.14118	– 0.23553
10	– 13.64156	1.82851	– 0.20101
11	– 13.26126	1.60326	– 0.17639
12	– 12.96479	1.41629	– 0.1557
13	– 12.75919	1.27432	– 0.14016
14	– 12.62833	1.1705	– 0.12912
15	– 12.4765	1.05481	– 0.11608
16	– 12.37305	0.96497	– 0.10616
17	– 12.31258	0.89712	– 0.09875
18	– 12.24943	0.82884	– 0.09113
19	– 12.19548	0.76602	– 0.08407
20	– 12.16014	0.71392	– 0.07827

The fits are valid over the temperature range of 2000K ≤ T ≤ 20 000 K. Also, it is possible that the fit is applicable outside this area but with caution. In the Table 2, the selected fits are presented (for $4 \leq n \leq 20$).

Relative contribution

$$A^*(n) + A \Rightarrow A_2^+ + e \qquad (4)$$

$$A^*(n) + A \Rightarrow A + A^+ + e \qquad (5)$$

$$A_2^+ + e \Rightarrow A^*(n) + A \qquad (6)$$

$$A + A^+ + e \Rightarrow A^*(n) + A \qquad (7)$$

Concurrent processes

$$A^*(n) + e \Rightarrow A^+ + 2e,$$

$$A^+ + 2e \Rightarrow A^*(n) + e,$$

$$A^+ + e \Rightarrow A^*(n) + \varepsilon_\lambda,$$

$$I_{\mathrm{ci}}(n, T) = K_{\mathrm{ci}}(n, T) \cdot N_n N_1,$$
$$I_{\mathrm{cr}}(n, T) = K_{\mathrm{cr}}(n, T) \cdot N_1 N_i N_e,$$

chemi-ionization/recombination fluxes

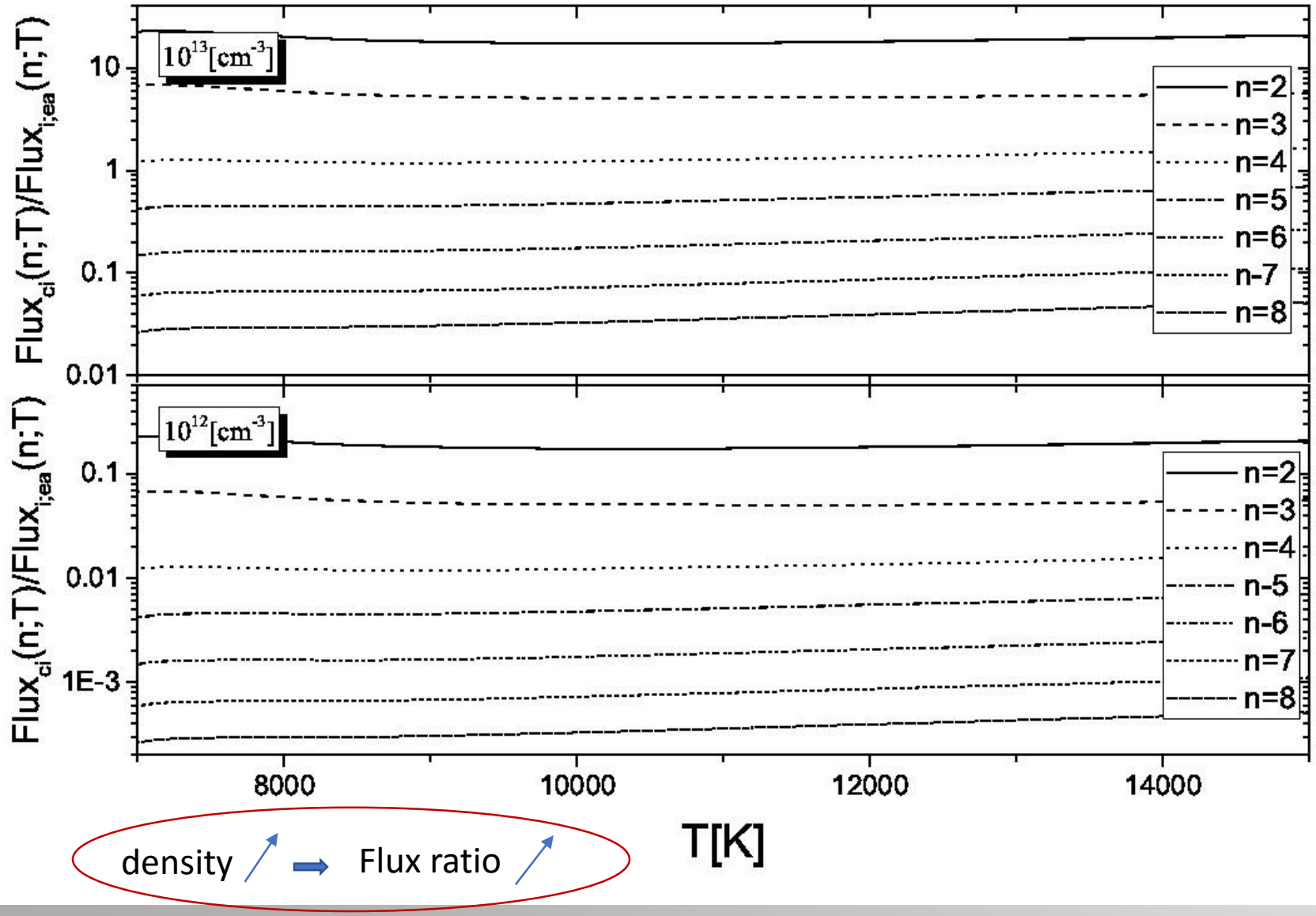

The influence of analyzed processes increases linearly with N, and, for example for $N = 10^{13}$ cm^{-3} some optical characteristics may be different than for $N = 10^{12}$ cm^{-3}.

Ratio of fluxes define the importance of CI

Namely, the influence of analyzed processes increases linearly with N, and, for example for $N = 10^{13}$ cm^{-3} some optical characteristics may be different than for $N = 10^{12}$ cm^{-3}, for example due to changes in energy level populations, electron density, influence on the formation of hydrogen molecule, opacity, line profiles etc.

We can see as well that even around the value of densities 10^{12} cm^{-3} the inclusion of the considered here chemi-ionization/recombination processes could improve the modelling and analysis of such regions not only in photospheres of Sun and solar like stars but also in clouds in AGN BLR.

Additionally, the Figure 3 demonstrates as well the high sensitivity of the influence of these processes to the relatively small changes of densities which can be of interest for the determination of limiting densities in clouds in AGN BLR.

It could be very useful to perform an analysis for example with the code CLOUDY in order to see which changes in optical characteristics may be used in order to establish the presence of such dense layers.

The results show that the considered chemi ionization/ recombination processes could be used for determination of limiting high densities in clouds in AGN BLR region and for the improvement of modelling of dense moderately ionized layers in them.

If exist changes in optical charact. (with inclusion ch.ion.)
=>
than there exists high densities in clouds in AGN BLR region

To conclude

The obtained results demonstrate the fact that the considered chemi-ionization/recombination processes, which influence on the ionization level and atom excited-state populations, must have a very significant influence on the optical properties of the weakly ionized regions where the neutral hydrogen densities are larger than 10^{12} cm^{-3} since in such conditions they dominate over the relevant concurrent electron–atom collision processes.

The possibility that the chemi-ionization processes in atom–Rydberg atom collisions, as well as the corresponding chemi-recombination processes, may be useful for the diagnostics, modelling, and confirmation of existence or non-existence of very dense weakly ionized domains in clouds in broad-line region of active galactic nuclei, has been considered.

Data are also useful for stellar plasma investigation:

This can be used as a diagnostic method to find out if the domains with such densities exist or not. Additionally, our previous results obtained for principal quantum number $2 \leq n \leq 8$ and $4000K \leq T \leq 10\,000K$ are extended for principal quantum number $9 \leq n \leq 20$ and $10\,000K < T \leq 20\,000K$ and also for low-temperature region ($T < 4000$ K) for $2 \leq n \leq 20$.

The results obtained during this investigation are in the process of inserting in our MolD molecular database which is web services at the Serbian virtual observatory (SerVO) and nodes within the Virtual Atomic and Molecular Data Center (VAMDC).

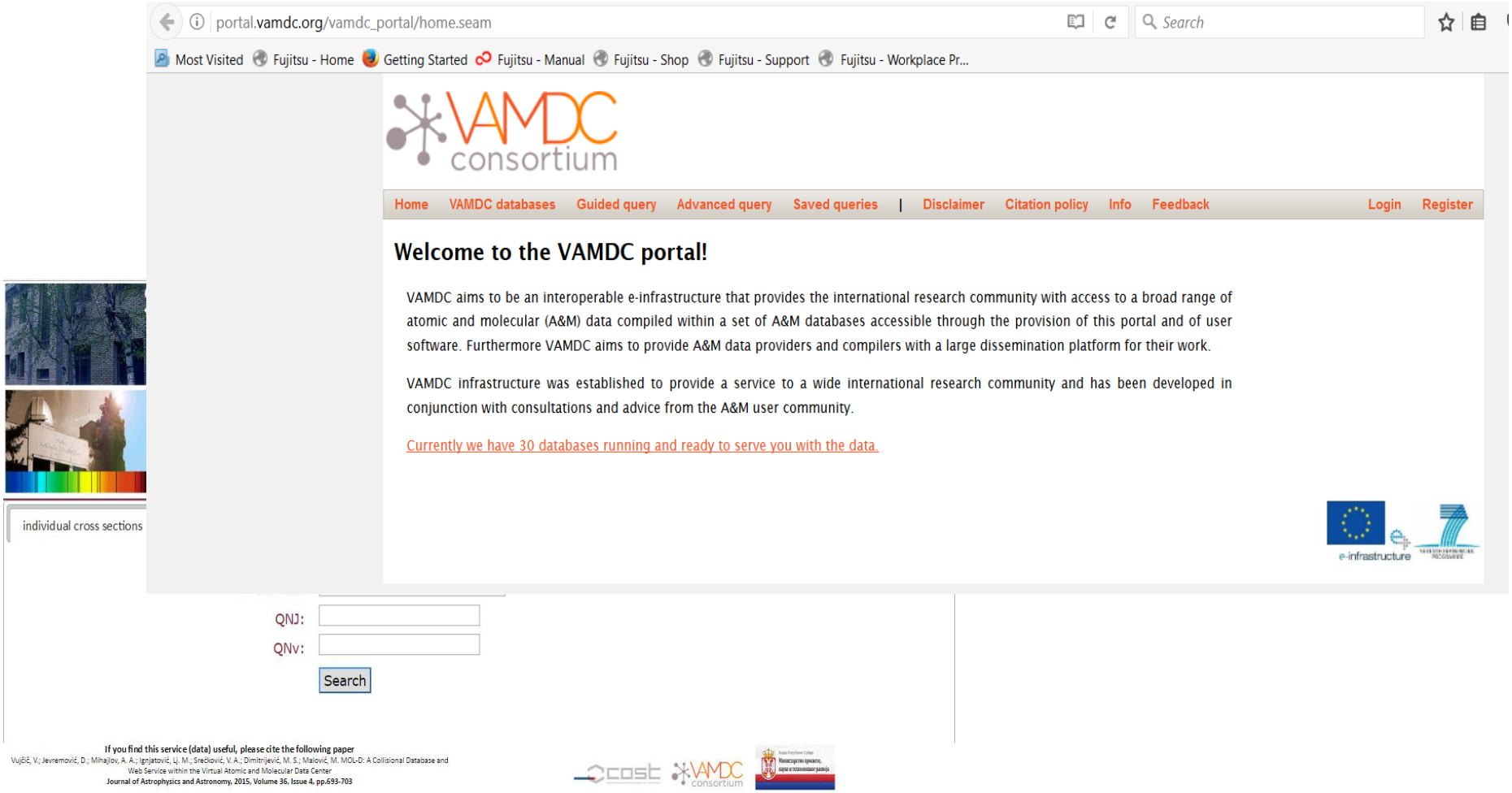

- VAMDC is consortium for sharing Atomic and Molecular data

- Currently 33 databases running in the consortium

ALADDIN2, BASECOL, Belgrade electron/atom(molecule) database (BEAMDB), CDMS, Carbon Dioxide Spectroscopic Databank 1000K, Carbon Dioxide Spectroscopic Databank 296K, Chianti, DESIRE, ECaSDa, S&MPO, GhoSST, HITRANonline, IDEADB, JPL database, KIDA, LXcat, MeCaSDa, OACT – LASP Database, PAH, Photodissociation - MolD database, RADAM - Ion Interactions, SHeCaSDa, SpEctroScopy of Atoms and Molecules Sesam, Spectr-W3, Stark-B, TFMeCaSDa, TIPbase, TOPbase, UMIST Database for Astrochemistry, VALD (atoms), VALD subset in Moscow, VAMDC species-DB, Water, …

- Large diversity among data

spectral line lists of atoms and molecules

transition probabilities

cross-sections (ro-vibrational, photodissociation, electron interaction…)

kinetic data

reaction rate coefficients

« Stark » broadening

VAMDC portal

- http://portal.vamdc.org/vamdc_portal/home.seam

Map of databases (on all continents)

THANK YOU FOR ATTENTION

The (n –n’)-mixing processes in the Broad Line Region of AGNs

Also in collisions H(n) + H(1s) i.e. Atom–Rydberg atom collisions we need to investigate excitation/de-excitation processes.

Our Future work => our current work. Next time talk in details.

excitation processes

$$\mathrm{H}^*(n) + \mathrm{H} \rightarrow \begin{cases} \mathrm{H}^*(n' = n + p) + \mathrm{H}, \\ \mathrm{H} + \mathrm{H}^*(n' = n + p), \end{cases} , \qquad n \geq 4, \quad p \geq 1, \quad (1)$$

and the inverse process of de-excitation

$$\mathrm{H}^*(n) + \mathrm{H} \rightarrow \begin{cases} \mathrm{H}^*(n' = n - p) + \mathrm{H}, \\ \mathrm{H} + \mathrm{H}^*(n' = n - p), \end{cases} \qquad n - p \geq 4, \qquad (2)$$

Table 2. Excitation rate coefficients $K_{n|n+p}(T)$ ($10^{-9}\mathrm{cm}^3\mathrm{s}^{-1}$). The values for $4 \leq n \leq 10$ and 3000 K $\leq T \leq$ 7000 K are from Mihajlov et al. (2004) and here are given for integrity.

		T[K]									
n	p	2000	3000	5000	7000	8000	9000	10000	15000	20000	25000
4	1	2.82409	4.42323	6.24561	7.18872	7.50148	7.74978	7.95119	8.56558	8.87458	9.05872
	2	0.32878	0.72276	1.32049	1.68755	1.81762	1.92380	2.01179	2.29039	2.43614	2.52470
	3	0.09004	0.24014	0.50917	0.69174	0.75905	0.81493	0.86185	1.01388	1.09539	1.14553
	4	0.03617	0.10906	0.25438	0.35948	0.39924	0.43261	0.46087	0.55383	0.60448	0.63590
	5	0.01806	0.05920	0.14738	0.21397	0.23960	0.26128	0.27975	0.34114	0.37496	0.39606
5	1	2.68161	3.37083	4.00610	4.29430	4.38513	4.45573	4.51208	4.67927	4.76096	4.80898
	2	0.50323	0.76422	1.04763	1.18951	1.23592	1.27255	1.30213	1.39164	1.43627	1.46275
	3	0.17648	0.30197	0.45344	0.53427	0.56137	0.58299	0.60057	0.65453	0.68182	0.69812
	4	0.08211	0.15238	0.24354	0.29437	0.31171	0.32563	0.33702	0.37231	0.39034	0.40116
	5	0.04510	0.08870	0.14824	0.18250	0.19433	0.20388	0.21172	0.23618	0.24877	0.25636
6	1	1.97872	2.24840	2.47312	2.56897	2.59849	2.62123	2.63924	2.69208	2.71760	2.73253
	2	0.47651	0.60719	0.72780	0.78249	0.79972	0.81311	0.82380	0.85548	0.87096	0.88005
	3	0.19300	0.26584	0.33798	0.37211	0.38304	0.39159	0.39844	0.41894	0.42904	0.43500
	4	0.09850	0.14346	0.19031	0.21317	0.22057	0.22639	0.23107	0.24517	0.25215	0.25629
	5	0.05765	0.08753	0.11985	0.13598	0.14125	0.14541	0.14876	0.15891	0.16396	0.16696
7	1	1.36415	1.47213	1.55736	1.59254	1.60324	1.61145	1.61792	1.63682	1.64590	1.65120
	2	0.38004	0.44152	0.49348	0.51583	0.52273	0.52805	0.53227	0.54466	0.55066	0.55417
	3	0.16853	0.20645	0.24012	0.25503	0.25969	0.26330	0.26617	0.27464	0.27875	0.28117
	4	0.09148	0.11660	0.13973	0.15020	0.15350	0.15606	0.15811	0.16417	0.16712	0.16886
	5	0.05597	0.07354	0.09018	0.09785	0.10028	0.10217	0.10368	0.10818	0.11038	0.11168

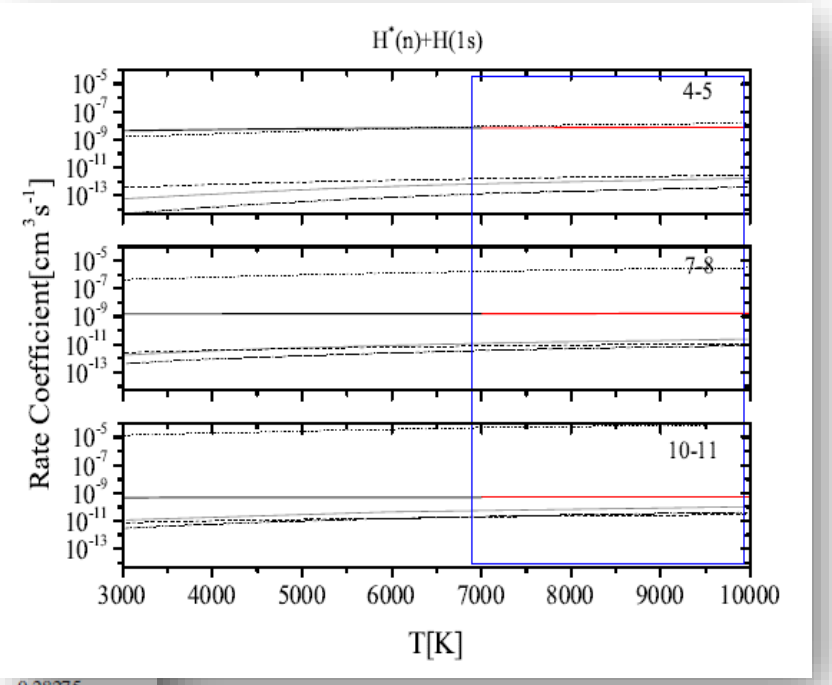

- We submitted in A&A

Astronomy & Astrophysics manuscript no. Dimitrijevic_et_al_A&A_corr2_2column
August 21, 2018

The $(n - n')$-mixing processes in the Broad Line Region of AGNs: data needed for spectroscopy diagnostics

Milan S. Dimitrijević[1,2,3], Vladimir A. Srećković[3,4], and Ljubinko M. Ignjatović[3,4]

[1] Astronomical Observatory Belgrade, Volgina 7, 11060 Belgrade, Serbia
[2] Observatoire de Paris, Sorbonne Université, Université PSL, CNRS, LERMA, F-92190 Meudon, France
[3] Isaac Newton Institute of Chile, Yugoslavia Branch, Volgina 7, 11060 Belgrade, Serbia
[4] University of Belgrade, Institute of Physics, P. O. Box 57, 11001 Belgrade, Serbia

e-mail: vlada@ipb.ac.rs
Received 06/11/2017; accepted 09/01/2018

The aim of our further investigation is to study the physics of AGN, i.e. to investigate the atomic processes (collisional atom - Rydberg atom i.e. chemi-ionization/recombination and n-n' mixing processes) and revise their role.

This means to find out at what plasma conditions certain atomic processes become important and could explain the existence of AGN regions with such characteristics, and could be used for future diagnostics, numerical simulations and modelling.

We will concentrate on:

- Calculations of the Balmer line ratios including chemi-ionization/recombination and n-n' mixing processes.
- Selection of the spectra of AGNs with broad emission lines in their spectra (type 1 AGN) where we expect that this process is dominant. The sample will contain more than 100 AGNs with high signal-to-noise ratio, from different databases (as e.g. SDSS database)
- Using different spectral tools we will fit the contininuum and broad emission lines (including Fe II optical broad lines) in order to get pure broad Balmer lines
- Comparison of the calculated and observed Balmer line ratios in order to extract the influence of chemi-ionization/recombination and n-n' mixing processes in the BLR.

- Srećkovic Vladimir vlada@ipb.ac.rs

Institute of Physics Belgrade, University of Belgrade, Serbia

<u>research interest</u>:

Solar and stellar astrophysics; High energy astrophysics; Atomic and ionic collisions with formation of quasimolecules; Atomic processes in white dwarfs and solar type stars; Astroinformatics; Databases; Space Weather studies of Upper Atmosphere; Ionospheric plasma Irregularities using VLF .

Also, people from the IF team: Lj.M. Ignjatović, A. Nina, N.Sakan …

AOB team i.e. collaborators in this thematic: Milan S. Dimitrijević, and others ….Darko Jevremović, Luka Popović, Zoran Simić, Veljko Vujčić

Astronomical Observatory, Belgrade, Serbia

collisional ionization